



miR-125b suppresses oral oncogenicity by targeting the anti-oxidative gene PRXL2A

Yi-Fen Chen^a, Yun-Yen Wei^a, Cheng-Chieh Yang^{a,b,c}, Chung-Ji Liu^{b,d}, Li-Yin Yeh^a,
Chung-Hsien Chou^a, Kuo-Wei Chang^{a,b,c,*}, Shu-Chun Lin^{a,b,c,**}

^a Institute of Oral Biology, National Yang-Ming University, Taipei, Taiwan

^b Department of Dentistry, National Yang-Ming University, Taipei, Taiwan

^c Department of Stomatology, Taipei Veterans General Hospital, Taipei, Taiwan

^d Department of Dentistry, MacKay Memorial Hospital, Taipei, Taiwan

ARTICLE INFO

Keywords:

HNSCC
miR-125
NRF2
Oxidation
Peroxiredoxin like 2A

ABSTRACT

Oral squamous cell carcinoma (OSCC) is a globally prevalent malignancy. The molecular mechanisms of this cancer are not well understood and acquire elucidation. Peroxiredoxin like 2A (PRXL2A) has been reported to be an antioxidant protein that protects cells from oxidative stress. Our previous study identified an association between PRXL2A upregulation in OSCC and a worse patient prognosis. MicroRNAs (miRNAs) are small non-coding RNAs that are involved in the modulation of biological/pathological properties. The miR-125 family of genes drive pluripotent regulation across a wide variety of cancers. In this study, we identify the oncogenic eligibility of PRXL2A and clarify miR-125b as its upstream regulator. Downregulation of miR-125b can be observed in OSCC tumors. Lower miR-125b expression in tumors results in a worse patient prognosis at the relatively early stage. Reporter assays are able to validate that PRXL2A is a direct target of miR-125b. Exogenous miR-125b expression in OSCC cells results in increased oxidative stress, increased drug sensitivity, and suppressor activity that is paralleled by the knockout of PRXL2A gene. The suppressor activity of miR-125b is able to be rescued by PRXL2A, which suggests the existence of a miR-125b-PRXL2A regulatory axis that is part of OSCC pathogenesis. Nuclear factor-erythroid 2-related factor 2 (NRF2) was found to be a downstream effector of the miR-125b-PRXL2A cascade. As a whole, this study has pinpointed novel clues demonstrating that downregulation of miR-125b suppressor underlies upregulation of PRXL2A in OSCC, and this then protects the affected tumor cells from oxidative stress.

1. Introduction

Head and neck squamous cell carcinoma (HNSCC), including oral squamous cell carcinoma (OSCC), is the sixth most common cancer worldwide [1,2]. Exposure to carcinogenic substances such as areca or tobacco, or to various viruses is the major etiological factors linked to OSCC [3,4]. Up to now, the five-year survival of OSCC has remained

low and this malignancy tends to relapse or progress even after treatment [5]. Therefore, it has become important to identify the molecular dis-regulation events that occur during OSCC in order to develop targets for therapy [6–8]. Reactive oxygen species (ROS) are intracellular chemical species that contain active oxygen atoms. Accumulated ROS causes oxidative stress and is known to induce cytotoxicity and genotoxicity in cells [9]. Cancer cells possess a higher tolerance to ROS than

Abbreviations: ANE, Areca nut extract; ARE, antioxidant response element; AUC, area under the curve; CDDP, cisplatin; CDS, coding sequence; C_t, threshold cycle; DNPH, 2, 4-Dinitrophenylhydrazine; FAM213A, Family with sequence similarity 213, member A; HNSCC, Head and neck squamous cell carcinoma; H₂O₂, hydrogen peroxide; IHC, Immunohistochemistry; ISH, In situ hybridization; miRNAs, MicroRNAs; NAC, N-acetyl-L-cysteine; NCMT, non-cancerous matched tissue; NRF2, Nuclear factor (erythroid-derived 2)-like 2; OS, overall survival; OSCC, Oral squamous cell carcinoma; PRX, Peroxiredoxin; PRXL2A, Peroxiredoxin like 2A; qPCR, quantitative PCR; ROC, receiver operating characteristic; ROS, Reactive oxygen species; Scr, scramble; TCGA, The Cancer Genome Atlas; TMA, tissue microarray; TRX, thioredoxin; wt, wild-type; 3'UTR, 3' untranslated region

* Corresponding author. Department of Dentistry, School of Dentistry, National Yang-Ming University, No. 155, Li-Nong St., Section 2, Taipei, 112, Taiwan. Tel.: +8862 28267223; fax: +8862 28264053.

** Corresponding author. Institute of Oral Biology, School of Dentistry, National Yang-Ming University, No. 155, Li-Nong St., Section 2, Taipei, 112, Taiwan. Tel.: +8862 28267272; fax: +8862 28264053.

E-mail addresses: ckcw@ym.edu.tw (K.-W. Chang), sclin@ym.edu.tw (S.-C. Lin).

<https://doi.org/10.1016/j.redox.2019.101140>

Received 17 October 2018; Received in revised form 22 January 2019; Accepted 8 February 2019

Available online 13 February 2019

2213-2317/ © 2019 The Authors. Published by Elsevier B.V. This is an open access article under the CC BY-NC-ND license (<http://creativecommons.org/licenses/by-nc-nd/4.0/>).

normal cells [10]. The nuclear factor-erythroid 2-related factor 2 (NRF2) plays an important role in maintaining cellular redox homeostasis [11]. Recent clues have identified that upregulation of NRF2 might help promoting survival and chemo-resistance in cancer cells [11]. In ovarian cancer, NRF2 has been shown to regulate cisplatin (CDDP) resistance through the activation of autophagy signaling [12]. In HNSCC cells, NRF2 was found to be overexpressed in more than 90% of tumors and the antioxidant response element (ARE)-activated CDDP resistance cells show reduced ferroptosis [11,13].

Peroxiredoxin (PRX) and thioredoxin (TRX) are two antioxidant protein families. The PRX enzymes contain an active cysteine site that is sensitive to oxidation by H₂O₂; whereas TRXs are redox proteins that catalyze the formation of disulfide bonds through a CXXC motif [14,15]. Peroxiredoxin like 2A (PRXL2A) gene is also called Family with sequence similarity 213, member A (FAM213A), C10orf58 or PAMM. It is an anti-oxidative protein that exhibits dual activities because it carries a PRX-like domain as well as an essential domain CXXC at the N-terminal that allows TRXs activation [14]. PRXL2A was identified during fetal liver development and is activated in M-CSF-stimulated monocytes [16]. The protein modulates osteoclast differentiation [17] and protects cells from oxidative stress; for example, it seems to be one of the antioxidants involved in the high-altitude adaptation by human populations living in the Andes, South America [18]. PRXL2A was found to be transcriptionally repressed by TCF12 in our previous study, and furthermore, its expression in OSCC tumors was found to be much higher than in non-cancerous matched tissue samples (NCMTs) in both humans and mice. Since the OSCC patients that were found to have strong PRXL2A expression also showed a trend towards worse survival [6], anti-PRXL2A strategies may be a feasible approach to improve OSCC therapy.

Notably, microRNAs are small noncoding RNAs that have been shown to regulate the translation and degradation of target mRNAs [19]. Among the most well-known miRNA families, *miR-125* family members are involved in a wide variety of cellular processes including cell differentiation, proliferation, metastasis, apoptosis, and immunological defense. The *hsa-miR-125* family consists of three homologous members *miR-125a*, *miR-125b-1* and *miR-125b-2*. Specifically, *miR-125a* is located at 19q13, while *miR-125b* has been verified to be transcribed from two loci, one located on chromosome 11q23 (*hsa-miR-125b-1*) and the other located on chromosome 21q21 (*hsa-miR-125b-2*) [20]. Although mature *miR-125a* and *miR-125b* have different sequences, they share the same seed sequence, which suggests that they are likely to regulate the same transcript targets [21].

The *miR-125* family members play pivotal roles in many different types of malignancies [20]. Compared to *miR-125a*, *miR-125b* has been much better studied. *miR-125b* is known to be downregulated in a broad variety of tumors and to regulate a range of different target genes involved in modulating oncogenic phenotypes, including migration, invasion, apoptosis, proliferation and colony formation [21]. For example, a low level of *miR-125b* has been found in carcinomas of bladder [22,23], breast [24,25], liver [26,27], ovary [28,29], as well as Ewing's sarcoma [30]. Raising *miR-125b* expression is known to reverse drug resistance in many types of cancers [31,32]. Circulating *miR-125b* can be used as a prognostic marker for the prediction of the recurrence and survival for several malignancies including OSCC patients [33–36]. In HNSCC, loss of *miR-125b* contributes to tumor development by targeting tumor-associated calcium signal transducer 2 and switching on MAPK signaling [37]. It is interesting to note in previous studies that NRF2 upregulates *miR-125b* expression in various types of cells by promoter activation [38–40]. However, the multi-dimensional regulatory mechanisms of *miR-125b* and the oncogenic stimuli leading to the *miR-125b* downregulation in OSCC are not fully understood [41–43].

In this study, we have investigated the oncogenic ability of PRXL2A and shown that *miR-125b* acts as its epigenetic upstream regulator. Exogenous *miR-125b* expression in OSCC cells was found to result in

increased ROS, increased CDDP sensitivity, and upregulation of suppressor activity; these were reversed by expression of PRXL2A. In addition, the *miR-125b*–PRXL2A cascade downregulates NRF2 expression in OSCC cells.

2. Materials and methods

2.1. Cell culture and reagents

The OSCC cell lines SAS, OECM1, HSC3, FaDu, and OC3 as well as Phoenix packaging cell, 293T cell and primary NOK cells were used in this study (Supplementary Table S1). Cell lines were obtained from either the ATCC or JCRB; alternatively they were derived according to previous published protocols [6]. Pilot tests validated the conditions for using miRVana™ *miR-125b* mimic, miRVana™ *miR-125b* inhibitor, miRVana™ scramble (Scr) control (Applied Biosystems, Foster City, CA) as well as Scr, siPRXL2A and siNRF2 oligonucleotides (Santa Cruz Biotech, Santa Cruz, CA) and these were identified to be 60 nM for 48 h. Areca nut extract (ANE) was prepared according to protocols previously described [4]. ANE (10, 25 or 50 µg/ml), arecoline (5 µg/ml) and nicotine (30 or 50 µg/ml) were used to treat cells for 2 h and acted as oncogenic stimuli. Hydrogen peroxide (H₂O₂; 2 mM) was used to induce ROS, while N-acetyl-L-cysteine (NAC; 70 mM) treatment was used to ameliorate a state where ROS was present. Unless specified, all other reagents were obtained from Sigma-Aldrich (St Louise, MO). The lipid transfection reagent Transfectin (BioRad Lab, Hercules, CA) was used for the transient expression system.

2.2. *miR-125b* and PRXL2A expression

The PRXL2A Human cDNA ORF (Clone number NM_032333 RC201327; OriGene Tech., Rockville, MD) was used as a template to create the PRXL2A constructs that were used in this study. The PRXL2A coding sequence (CDS) and this CDS plus a portion of the 3' untranslated region (3'UTR) that contains the predicted *miR-125b* and *miR-4319* target site were cloned into the pBABE-puro retroviral vector. After retroviral infection and puromycin selection, stable SAS cell subclones expressing PRXL2A were obtained and these were designated CDS and CDS + 3', respectively. Cell subclones that were expressing the vector only were also created and these control cells were designated VA. The pre-*miR-125b* sequence was cloned into pLAS5w.PtRFP-I2-puro vector (National RNAi Core, Academia Sinica, Taipei, Taiwan). After lentiviral infection and puromycin selection, a stable SAS subclone expressing *miR-125b* was identified and designated S*miR-125b*. S*miR-125b* and a SAS subclone that was expressing vector alone (designated SVA) were both able to express red fluorescence, which could be detected under fluorescence microscopy. The primers used to amplify relevant sequences are listed in Supplementary Table S2. The plasmid NRF2 CDS in pBABE-neo vector was a gift from Professor Yang, Cheng-Chieh.

2.3. PRXL2A knockout

The pAll-PRXL2-Cas9-Ppuro vector was purchased from National RNAi Core. This vector co-expresses Cas9 and sgRNA that targets PRXL2A. The pSurrogate vector (National RNAi Core) containing a sgRNA-target segment sandwiched between an out-of-frame mCherry cassette and an in-frame enhanced GFP cassette was used as the reporter. Cells, co-transfected with both vectors, exhibited green fluorescence. Red fluorescence could also be observed in cells that had been effectively modified because of the Cas9/PRXL2 sgRNA. SAS cells with red fluorescence were sorted and enriched. DNA was isolated from these subclones in order to detect the mutations by sequencing. The PRXL2A knockout SAS cell subclone was designated KO.

2.4. Reporter construction and assay

The miRNA target sites within the PRXL2A 3'UTR was predicted by miRWalk software (<http://mirwalk.umm.uni-heidelberg.de/>; Supplementary Table S3). Regions of the PRXL2A sequence that encompassed either the wild-type (wt) or mutant (mut) *miR-125b* target site were cloned into the pMIR-REPORT™ luciferase reporter vector (Applied Biosystems). The mut plasmid was obtained from the wt plasmid by replacing the *miR-125b* targeted sequence CUCAGGGA with ACGCGT, a *MluI* restriction enzyme digestion site. The PCR primers used are listed in Supplementary Table S2. The Dual-Luciferase® Reporter (DLR™) Assay System (Promega, Madison, WI) was used to detect reporter activity and the measurements were carried out by normalizing the firefly luciferase activity against the renilla luciferase activity.

2.5. Quantitative PCR analysis

All RNAs were isolated using Tri-reagent (Molecular Research Center, Cincinnati, OH) according to the manufacturer's protocol. The collection of the tissue samples used in this study (Supplementary Table S4) was approved by the Institutional Review Board with Approval No. 15MMHIS105. The expression of *miR-125* was analyzed using the TaqMan MicroRNA Assay system (Applied Biosystems) with *RNU6B* as an internal control. The expression of *PRXL2A* was analyzed by the TaqMan qPCR Assay system (Applied Biosystems) with *GAPDH* as the internal control. The TaqMan® assay probes are listed in Supplementary Table S5. The relative changes in gene levels were determined by the threshold cycle (C_t) method. The $2^{-\Delta\Delta C_t}$ values were used to represent the fold change in the experimental groups compared to the control groups.

2.6. Western blot analysis

Cell lysates were separated by 10% polyacrylamide gel electrophoresis according to previously described protocols [6,7,44,45]. *GAPDH* was used as the internal control for quantification of the various proteins. The primary and secondary antibodies are described in Supplementary Table S6. The cellular oxidative proteins were analyzed using the Oxidized Protein Western Blot Kit (Abcam, Cambridge, MA) according to the manufacturer's protocol. This assay detected carbonyl-containing 2, 4-Dinitrophenylhydrazine (DNPH) adducts after DNPH was added in a reaction that involved the presence of oxidized proteins.

2.7. Phenotype and tumorigenesis assays

Cell proliferation ability was analyzed by MTT assay. The assays measuring migration and invasion, as well as to measure anchorage-independent colony formation by cells followed previous protocols [6,44,45]. To carry out xenografic tumorigenesis, 5×10^5 cells were injected subcutaneously into the flank of 6-week to 8-week-old athymic mice (National Laboratory Animal Center, Taipei, Taiwan). The tumors were measured twice a week and the mice were sacrificed at the end of the third week. Tumor volumes were calculated using the formula volume = $0.5 ab^2$, where *a* and *b* are the longest and shortest diameters of the tumors. The animal study was approved by the Institutional Animal Care and Use Committee of National Yang-Ming University.

2.8. ROS assay

Cultivated cells were challenged with 2 mM H_2O_2 at 37 °C for 30 min or not, then they stained with 25 μ M CM- H_2 DCFDA (Invitrogen, Carlsbad, CA) at 37 °C for 30 min. After trypsinization and washing, the intensity of DCF fluorescence inside the cells was analyzed by FACSCalibur™ flow cytometer (BD Biosciences, Franklin Lakes, NJ).

2.9. Immunohistochemistry (IHC) and in situ hybridization (ISH)

The paraffin-embedded human OSCC tissue microarray (TMA) sections used in this study were approved for use by the Institutional Review Board with an approval no. of 2013-11-011B. The antibodies for IHC are listed in Supplementary Table S6. The miRCURY LNA™ hsa-*miR-125b-5p* probe #190442 was labeled with digoxigenin and then used for the ISH. All associated reagents for ISH analysis were purchased from Exiqon (Copenhagen, Denmark). The tissue staining signals were quantified by pixel scores using Photoshop software (Adobe; San Jose, CA) [6,44].

2.10. Statistical analysis

Data are presented as means \pm SE. Disease status was determined using receiver operating characteristic (ROC) analysis, and the area under the curve (AUC) was used to test discriminative ability. The following statistical methods, *t*-tests, two-way ANOVA testing, correlation tests and Kaplan–Meier survival analysis, were used to compare the differences in overall survival (OS) between groups. A *p*-value of less than 0.05 was considered statistically significant. *ns*, not significant; *, *p* < 0.05; **, *p* < 0.01; ***, *p* < 0.001.

3. Results

3.1. PRXL2A is a direct target of miR-125b in OSCC cells

Oncogenic stimuli, consisting of treatment with ANE, arecoline, and nicotine for 2 h, resulted in a pronounced upregulation of PRXL2A in SAS cells (Fig. 1A). We performed an *in silico* analysis and searched for miRNAs that might target PRXL2A. Three, *miR-125a/b*, *miR-4319*, and *miR-7*, were shown to have potential as miRNAs targeting PRXL2A, targets various different sites in the 3' UTR of the gene (Supplementary Table S3). qPCR analysis showed that there was an increased expression of PRXL2A in various OSCC cell lines, namely SAS, OECM1, HSC3, OC3, and FaDu, compared to the NOK cell (Fig. 1B). *miR-125a* expression levels were not consistently different across these OSCC cells. However, *miR-125b* expressions were consistently downregulated in these OSCC cell lines compared to the NOK cell (Fig. 1C). Thus, a negative correlation between the *miR-125b* expression and PRXL2A mRNA expression was identified in relation to various types of oral keratinocytes (Fig. 1D). *miR-7* expression was upregulated in OSCC cell lines relative to NOK cell. The *miR-4319* expression levels in OSCC cell lines were not consistent (Supplementary Fig. S1A). A correlation between the *miR-7* expression and PRXL2A expression was identified in oral keratinocytes. Besides, there was no correlation lying between *miR-4319* expression and PRXL2A expression (Supplementary Fig. S1B).

Downregulation of PRXL2A mRNA expression and PRXL2A protein expression was found in SAS and FaDu cells that had been treated with the *miR-125b* mimic (Fig. 1E). By way of contrast, cells treated with *miR-125b* inhibitor showed upregulation of PRXL2A expression (Fig. 1F). The downregulation of PRXL2A protein expression brought about by the *miR-125b* mimic was rescued by *miR-125b* inhibition (Fig. 1G). To elucidate whether *miR-125b* represses PRXL2A by directly targeting the gene's 3'UTR, we generated wt PRXL2A reporter and mut PRXL2A reporter systems. Supplementary Fig. S2A illustrates the complementarity between the PRXL2A 3'UTR sequence and *miR-125b*. *miR-125b* expression was found to repress the activity of the wt reporter while such repression did not occur with the mut reporter (Fig. 1H). The same reporters were used to assay the targeting of *miR-4319* on PRXL2A (Supplementary Fig. S2B). *miR-4319* expression was unable to affect the reporter activities (Supplementary Fig. S3). The Western blot analysis demonstrated both the CDS and the CDS + 3' subclones had higher levels of PRXL2A expression relative to VA, and the CDS had a higher level of PRXL2A expression than CDS + 3' (Fig. 1I). It seems likely that endogenous *miR-125b* is also able to repress exogenous

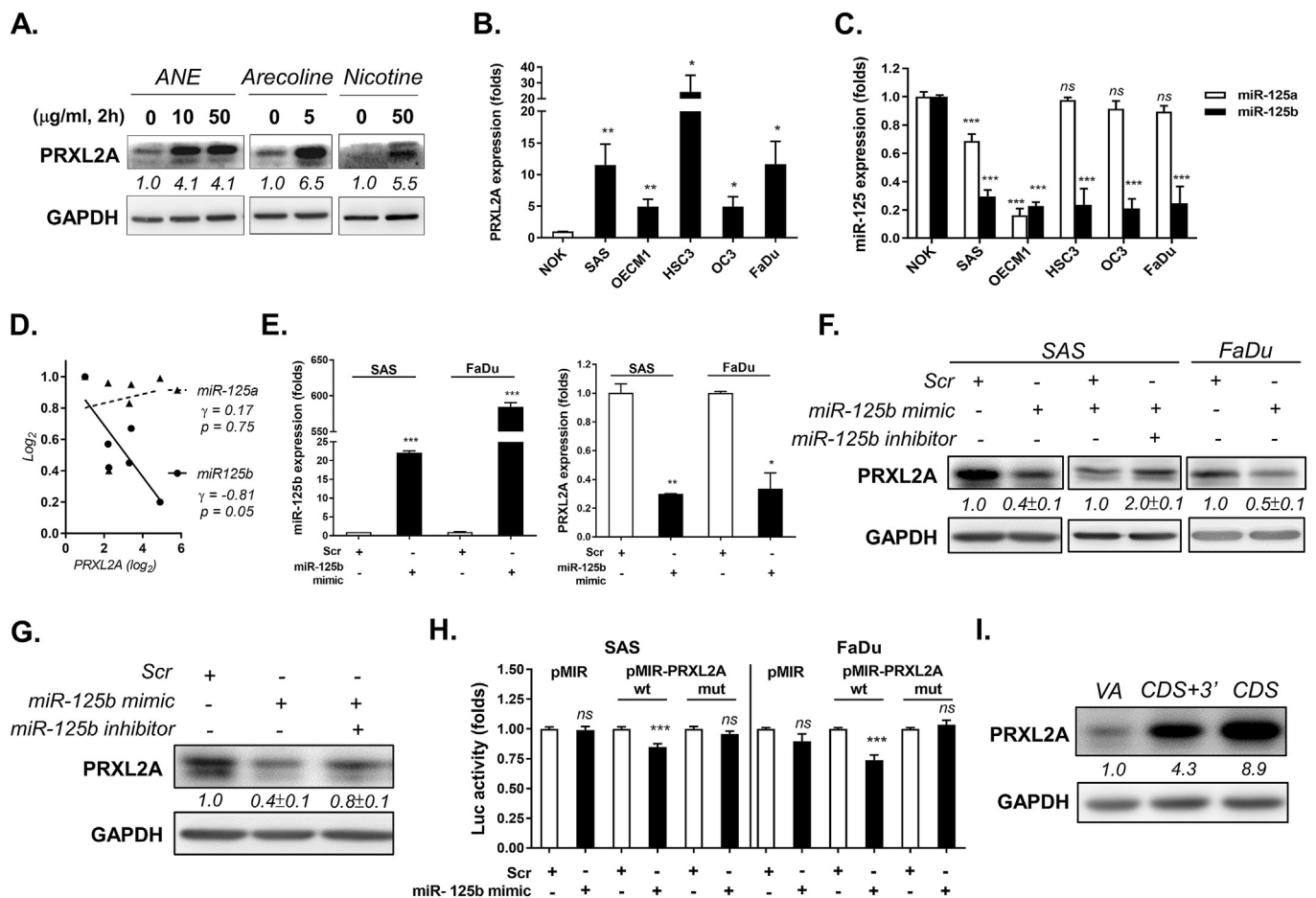


Fig. 1. *miR-125b* targets *PRXL2A* in OSCC cells. A, F, G, I. Western blot analysis. B, C, E. qPCR analysis. A, G, I. SAS cell line. A. ANE, arecoline and nicotine induce *PRXL2A* expression. B. *PRXL2A* mRNA expression in OSCC cell lines. C. *miR-125a/b* expression in OSCC cell lines. D. Correlation analysis. Negative correlation is present between *miR-125b* expression and *PRXL2A* expression in OSCC cells. E. Left, *miR-125b* expression; Right, *PRXL2A* mRNA expression. E, F. Downregulation of *PRXL2A* mRNA expression and protein expression in SAS and FaDu cells in the presence of *miR-125b* expression. F. Inhibition of *miR-125b* upregulates *PRXL2A* protein expression in the SAS cell expressing *miR-125b*. G. Downregulation of *PRXL2A* expression in cells with *miR-125b* expression is rescued by *miR-125b* inhibition. H. Reporter assay. *miR-125b* expression represses the wt reporter, but it has no effect on the mutant reporter. I. *PRXL2A* expression. Both the CDS + 3' and CDS subclones have higher *PRXL2A* expression than the control. Moreover, the CDS subclone has higher *PRXL2A* expression than the CDS + 3' subclone. wt, wild-type; mut, mutant. Numbers below pictures, normalized values. Data shown in F. and G. are mean \pm SE from quadruplicate analysis.

PRXL2A protein expression by targeting the 3'UTR sequence in CDS + 3' subclone. These results support the hypothesis that, in OSCC, *miR-125b* is able to repress *PRXL2A* expression by direct targeting the 3'UTR of *PRXL2A*.

3.2. *PRXL2A* drives various oncogenic processes present in SAS cells

The CDS subclone was found to exhibit increased *PRXL2A* protein expression and the increase was about 10 fold (Fig. 2A). *PRXL2A* deficient mutant subclones were generated by gene editing and were named KO_1 to KO_6. Western blot analysis showed that there was an absence of *PRXL2A* expression in four of them (Fig. 2B). When subclones KO_1 and KO_6 were sequenced, base deletions were detected that resulted in frameshifts and thus truncation of the encoded protein (Supplementary Fig. S4); the end result was the absence of *PRXL2A* protein signals. The presence of *PRXL2A* protein expression increased the oncogenic characteristics of SAS cells, including proliferation, migration, invasion, and colony formation (Fig. 2C). By way of contrast, the KO_6 subclone displayed remarkable decreases in these properties (Fig. 2D). As *PRXL2A* is a ROS modulator and the creation of carbonyl groups on proteins is a marker of oxidative stress [6], we carried out an assay showed that *PRXL2A* expression decreased the presence of carbonyl proteins (Fig. 2E). Flow cytometry analysis also showed that

expression of *PRXL2A* decreased the intracellular level of ROS (Fig. 2F). The CDS + 3' subclone had a lower level of *PRXL2A* expression compared to the CDS subclone, and importantly, this correlated with lower levels of the migration and invasion by the CDS + 3' subclone than the CDS cell subclone (Supplementary Figs. S5A and B). Furthermore, the stimulation of ROS found in the CDS + 3' subclone was higher than in the CDS subclone (Supplementary Fig. S5C). CDDP is one of the most widely used anticancer drugs and can target several types of tumors, including OSCC. CDDP-generated cytotoxicity has been correlated with the presence of a mitochondrial ROS response and binding of the drug to guanine bases in DNA [46]. The *PRXL2A* KO subclones were found to have higher CDDP sensitivity than the parental cell (Fig. 2G). In agreement with this, the CDS subclone exhibited higher CDDP resistance than the CDS + 3' or VA subclones due to the former's higher level of *PRXL2A* expression (Supplementary Fig. S5D). Exogenous *PRXL2A* expression in cells was found to enhance subcutaneous tumor growth of SAS cell, while the *PRXL2A* KO subclones showed significantly reduced xenographic growth (Fig. 2H). Specifically, exogenous *PRXL2A* expression was able to increase the weight and volume of SAS xenografts by about two-fold (Supplementary Fig. S6A). Furthermore, the silencing of *PRXL2A* expression was able to drastically decrease the xenographic tumor burden to about one-quarter of the control tumors (Supplementary Fig. S6B). These results support the hypothesis that

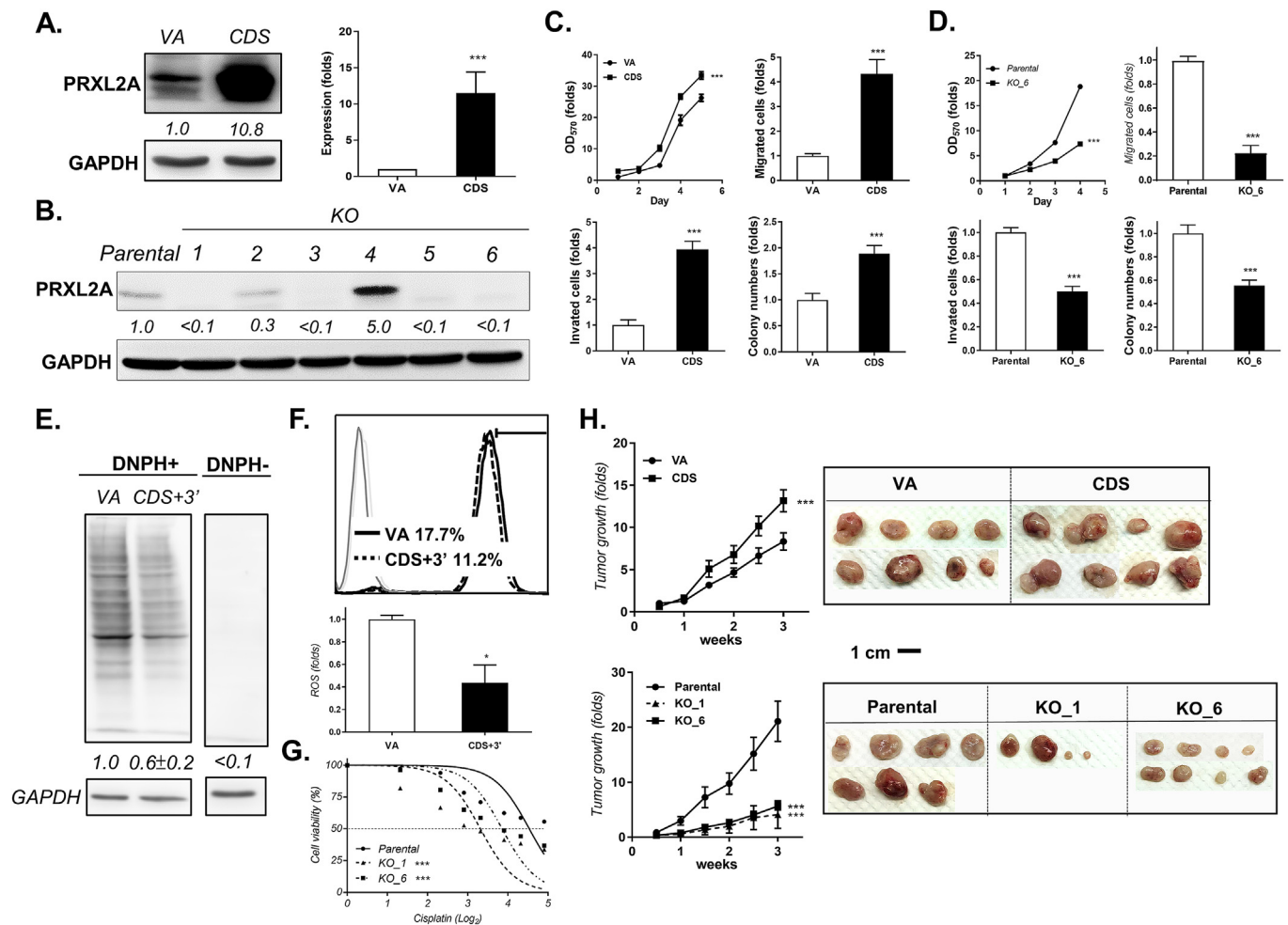


Fig. 2. PRXL2A mediates oncogenic activity in the SAS cell line. A, B, E. Western blot analysis. A. PRXL2A expression. Left, gel image; Right, quantification. The CDS subclone exhibits increased PRXL2A protein expression. B. PRXL2A deficiency. The PRXL2A knockout subclones KO_1 and KO_6 subclones are absent of PRXL2A expression and selected for further study. C, D. Phenotypic assays of CDS and KO. Left upper, proliferation; Right upper, migration; Left lower, invasion; Right lower, anchorage-independent colony formation. C. The enriched oncogenic phenotypes present in the CDS subclone. D. The reduced oncogenic phenotypes present in the KO_6 cell subclone. E. Increased antioxidant enzyme activity in CDS + 3' subclone as shown by the reduction in DNP adducts. F. ROS assay. Upper, flow cytometry diagram; Lower, quantification. A decrease in ROS in CDS + 3' cell subclone can be seen. G. Dose-response curve following CDDP treatment. The KO subclones exhibit increased CDDP sensitivity relative to the parental cells. H. Subcutaneous tumorigenesis. Upper, CDS subclone and control; Lower, KO subclones and parental cells; Left, growth curve; Right, resected tumors. The level of PRXL2A expression associates with the xenographic growth potential of the SAS cells. Numbers below pictures, normalized values. Data shown in E. are mean \pm SE from triplicate analysis.

PRXL2A expression in SAS cells contributes to oncogenesis, tumorigenesis, ROS scavenging and chemo-resistance.

3.3. miR-125b expression suppresses oncogenicity, increases ROS and sensitizes SAS cell

SAS cells were treated with miR-125b mimic, and qPCR analysis was carried out; this revealed that there was upregulation of miR-125b expression (Fig. 1E). The increase in miR-125b expression reduced the oncogenic phenotypes, including proliferation (Fig. 3A), migration (Fig. 3B) and invasion (Fig. 3C). The increase in miR-125b expression resulted in higher levels of protein oxidation as revealed by the detection of more carbonylated protein (Fig. 3D). miR-125b expression also increased the intracellular ROS levels in OSCC cells (Fig. 3E). We generated a SmiR-125b subclone from SAS cells and both the SmiR-125b and SVA subclones showed red fluorescence (Supplementary Fig. S7A); furthermore, miR-125b expression was found to be increased by about 10 folds in the SmiR-125b subclone relative to SVA (Supplementary Fig. S7B). The presence of exogenous miR-125b expression was also able to attenuate colony formation by SAS cells (Fig. 3F). These cells also

showed a slight increase in ROS (Supplementary Fig. S7C) and CDDP sensitivity (Fig. 3G).

3.4. miR-125b associated tumor suppression, ROS induction and cisplatin sensitivity is mediated via targeting of PRXL2A

To unravel the functional effects of the miR-125b-PRXL2A cascade, transient co-expression of miR-125b and PRXL2A was carried out. The analysis revealed that the miR-125b was able to bring about reduced migration (Fig. 4A), reduced invasion (Fig. 4B) and less colony formation (Fig. 4C), and these could be rescued by expression of PRXL2A. The intracellular levels of ROS were increased by miR-125b but decreased by expression of PRXL2A (Fig. 4D). Drug sensitivity test showed that miR-125b associated CDDP sensitivity was reversed by expression of PRXL2A (Fig. 4E). A retrieval of the gene expression profiles of various antioxidants, including GSTP1, GPX1/2, NRF2, GSTM, CAT, and SOD2, from The Cancer Genome Atlas (TCGA) HNSCC tissue database showed that expression level of PRXL2A to be positively correlated with the expression levels of GSTP1, GPX1/2, NRF2 and GSTM (Fig. 4F).

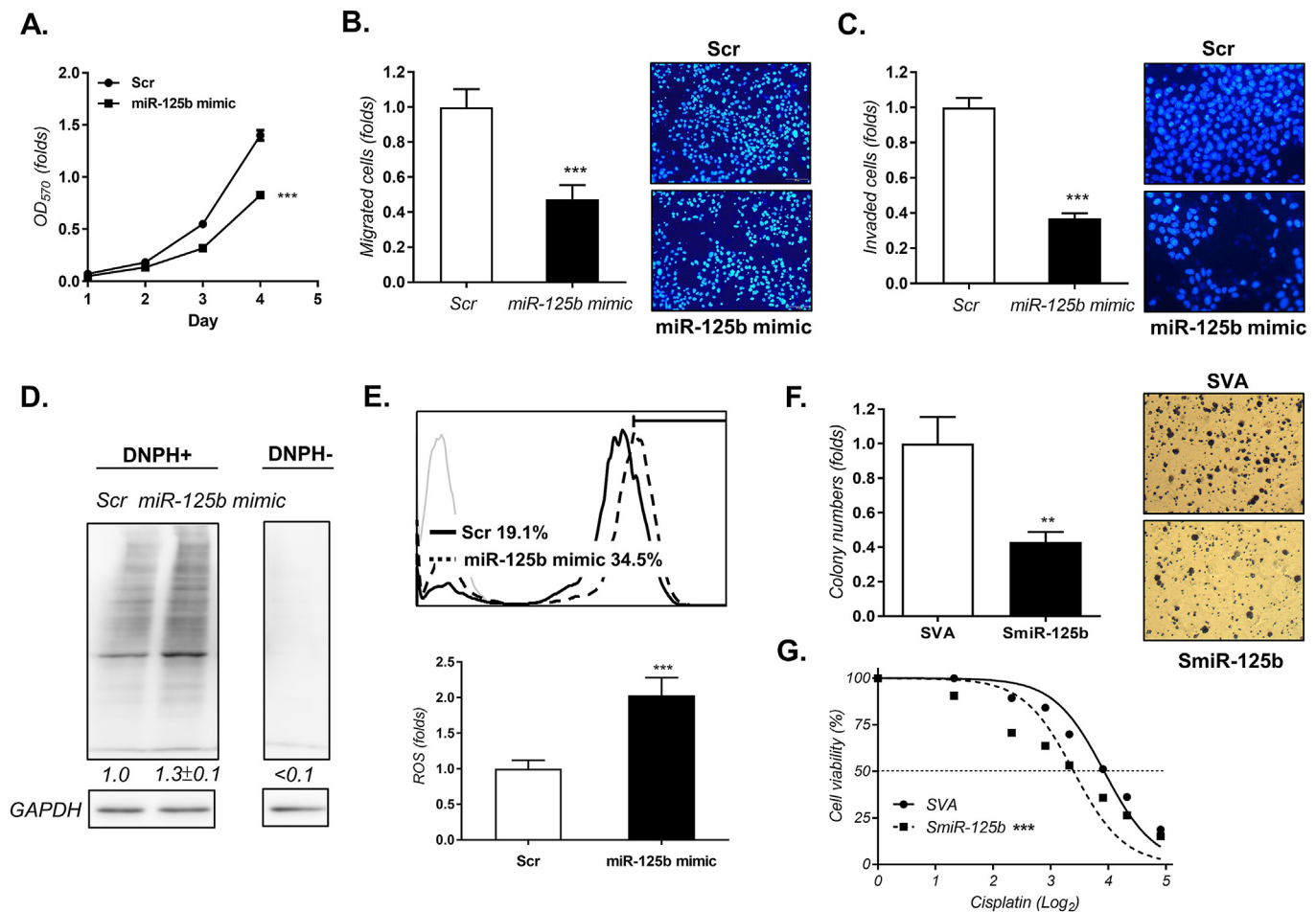


Fig. 3. *miR-125b* mediates suppressive activity in the SAS cell line. A – C, F. Phenotypic assays including proliferation, migration, invasion, and anchorage-independent colony formation. B, C, F. Left, quantification; Right, representative assay fields. A – E. Exogenous *miR-125b* expression following treatment with the *miR-125b* mimic. F, G. Analysis of the *SmiR-125b* subclone and the SVA control. A – C, F. *miR-125b* expression is associated with decreased oncogenicity. D. Western blot analysis. *miR-125b* expression increases the amount of DNP adducts detected. E. ROS assay. Upper, flow cytometry diagram; Lower, quantification. *miR-125b* expression increases intracellular ROS. G. Dose-response curve following CDDP treatment. Increased CDDP sensitivity is present in the *SmiR-125b* subclone relative to the control. Numbers below pictures, normalized values. Data in D. are mean \pm SE from triplicate analysis.

3.5. NRF2 is a downstream effector of PRXL2A in OSCC cells

NRF2 expression in OSCC cell lines was generally higher than NOK (Supplementary Fig. S8A). The NRF2 expression was in trends of positive correlation with PRXL2A expression, and negative correlation with *miR-125b* expression (Supplementary Fig. S8B). In SAS cell, a remarkable increase in the level of NRF2 in the CDS subclone, and a slight decrease of NRF2 in the KO_1 and *SmiR-125b* subclones was noted (Fig. 5A). There was also an increase levels of GSTP1 and GPX1/2 in the CDS subclone and a decrease levels of these in the KO_1 and *SmiR-125b* subclones. However, the changes in the level of other antioxidants were not consistent across the various subclones (Fig. 5A). Transient exogenous expression of NRF2 and knockdown of NRF2 were found not to affect PRXL2A expression (Fig. 5B). Nevertheless, PRXL2A expression did increase NRF2 expression, and this increase was reduced in the presence of siNRF2 (Fig. 5C). HSC3 and FaDu cells transfected with PRXL2A CDS showed increased levels of NRF2 expression (Fig. 5D, left), while HSC3 and OECM1 cells transfected with siPRXL2A showed decreased of NRF2 expression (Fig. 5D, right). In SAS cells treated with ANE and nicotine for 2 h, both PRXL2A and NRF2 expression were found to be upregulated. In contrast, in the KO subclones, the upregulation of NRF2 following oncogenic stimulation was less obvious (Fig. 5E and F, left). Transient knockdown of PRXL2A decreased NRF2 in SAS cell. In SAS cells with oncogenic stimulation, both PRXL2A and

NRF2 were upregulated (Fig. 5E and F, middle). NRF2 upregulation following oncogenic stimuli was less obvious in PRXL2A knockdown cells. In HSC3 and FaDu cell lines, ANE or nicotine treatment upregulated both PRXL2A and NRF2 (Fig. 5E and F, right). Collectively, the results indicated that PRXL2A would seem to be a crucial downstream effector of *miR-125b*, and its abundance then affects the expression of a panel of antioxidant enzymes, especially NRF2. To address if NRF2 regulates *miR-125* expression, NRF2 expression and knockdown were performed in NOK and OSCC cell lines. The analysis showed an absence of consequential changes of *miR-125a* or *miR-125b* expression following the fluctuation of NRF2 expression in oral keratinocytes (Supplementary Fig. S9).

3.6. Association between PRXL2A and *miR-125b* expression in human OSCC tissues

To understand the expression status and the prognostic values of *miR-125b* and PRXL2A in oral carcinogenesis, qPCR, IHC and ISH analysis were performed on human OSCC tissues. ROC analysis based on the qPCR results indicated that *miR-125b* expression had a separation power of 0.814 when distinguishing OSCC from NCMT (Fig. 6A). In addition, *miR-125b* expression was shown to decrease following the growth of primary tumors from the earlier stage ones to the later stage ones (Fig. 6E). Quantification of the pixel readings in TMA revealed

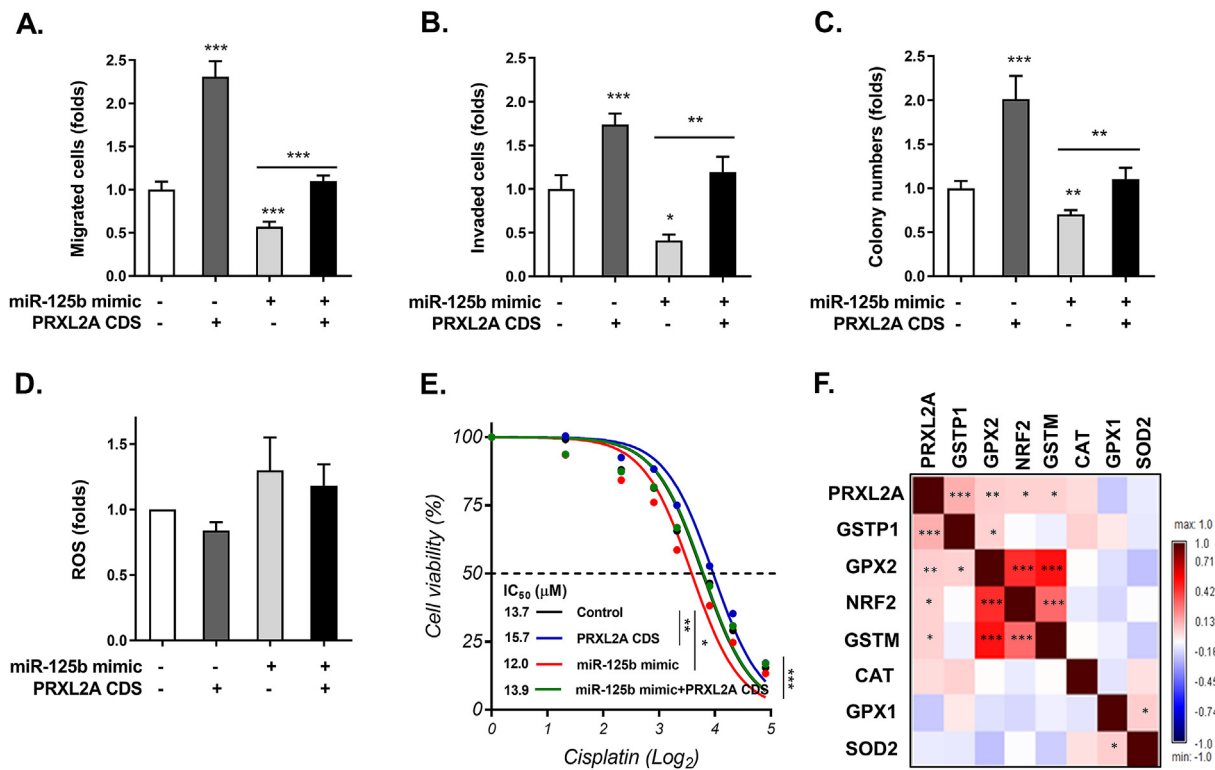


Fig. 4. PRXL2A expression rescues *miR-125b* mediated oncogenic suppression. A – E. Exogenous *miR-125b* and PRXL2A expression in SAS cells carried out by transfecting the *miR-125b* mimic and PRXL2A CDS constructs. A – C. Phenotypic assays including migration, invasion, and anchorage-independent colony formation. D. ROS assay. Repeat analyses were performed. No statistical analysis was carried out. E. The dose-response curve following CDDP treatment. A – E. Oncogenic suppression, ROS induction and CDDP sensitivity following *miR-125b* expression are able to be rescued by PRXL2A expression. F. Heatmap algorithm. Expression correlations between PRXL2A and antioxidant genes were found to be presented in the TCGA HNSCC database. There are also strong correlations among the expression levels of NRF2, GPX2, and GSTM. Gradient bar, γ value.

there was increased PRXL2A immunoreactivity in OSCC tumors relative to NCMT samples. ROC analysis further showed that PRXL2A immunoreactivity had a predictive power of 0.932 when distinguishing OSCCs from NCMTs (Fig. 6D). Representative tumors (Fig. 6C) and correlation analysis were able to demonstrate a negative correlation between *miR-125b* staining and PRXL2A immunoreactivity (Fig. 6B) in OSCC of TMA. Low *miR-125b* expression in tumors was associated with a trend towards worse OS of patients (Supplementary Fig. S10A). In the subset of patients who were at relatively earlier stages (stage I – III) of OSCC and low *miR-125b* expression defined a worse prognosis (Fig. 6F). The expression of *miR-125b* was unable to predict the OS in stage IV patients (Supplementary Fig. S10B). Analysis using the combination of *miR-125b* and PRXL2A staining also indicated that the presence of low *miR-125b* expression and high PRXL2A expression in a tumor was associated with a trend towards lower OS relative to their counterparts (Supplementary Fig. S10C). The nodal status of our patient cohort was associated with OS. But the analytical power is marginal (Supplementary Fig. S10D). However, when the patient subset having nodal involvement was investigated, low *miR-125b* expression and high PRXL2A expression in tumors displayed a very low survival rate (Fig. 6G). *miR-125b* staining and PRXL2A immunoreactivity were not associated with other clinicopathological parameters.

4. Discussion

In a previous study, we have shown that the *miR-211*-TCF12 oncogenic axis in OSCC is able to upregulate PRXL2A expression by transcriptional activation. PRXL2A (also named FAM213A previously) is highly associated with the aggressive properties of OSCC and it would seem to help protect cancer cells from oxidative damage. Moreover, a majority of OSCC tissue samples have been found to have strong

PRXL2A expression, and this is associated with the early establishment of tumorigenesis [6]. Herein, we clarify post-transcriptional repression of PRXL2A expression via direct targeting by *miR-125b*. *miR-125b* downregulation is another mechanism that can lead to higher levels of PRXL2A expression in tumors. Coordination of *miR-211* upregulation and *miR-125b* downregulation thus may drive OSCC oncogenesis. While downregulation of *miR-125b* expression has been identified in HNSCC [36,43], upregulation of *miR-125b* expression in HNSCC has also been reported [42]. Our results demonstrate there is a concordance between low *miR-125b* expression and high PRXL2A expression in OSCC cell lines and various tumor tissues. *miR-7* is frequently upregulated in OSCC tumors [47], this study also identifies the high *miR-7* expression in OSCC cell lines. Thus, it is unlikely that *miR-7* would target PRXL2A since they are concordant in expression. Whether the lack of targeting efficiency of *miR-4319* is ascribed to its shortness in length requires specification. Despite the fact that *miR-125b* downregulation has been shown to be a predictor of poor survival among late-stage OSCC in other studies [36], our preliminary analysis notes here that while such downregulation of *miR-125b* takes place during the enlargement of tumor mass, it could be further validated by multivariate analysis as a potential prognosticator in relatively early tumors. This study also finds that OSCC patients with low *miR-125b* expression and high PRXL2A expression together with the nodal involvement have a very poor survival rate. But since the sample size of this study is small, the findings need to be confirmed in larger patient cohorts.

The *miR-125* family members play versatile roles in the modulation of various pathophysiological processes including HNSCC pathogenesis [20,36,37,43,48]. *miR-125b* has been reported to suppress Notch1 and p63 expression as well as promoting Hailey–Hailey disease in association with oxidative stress [49]. In ovarian cancer, ROS seems to play a role in the induction of DNMT1 expression, which then downregulates

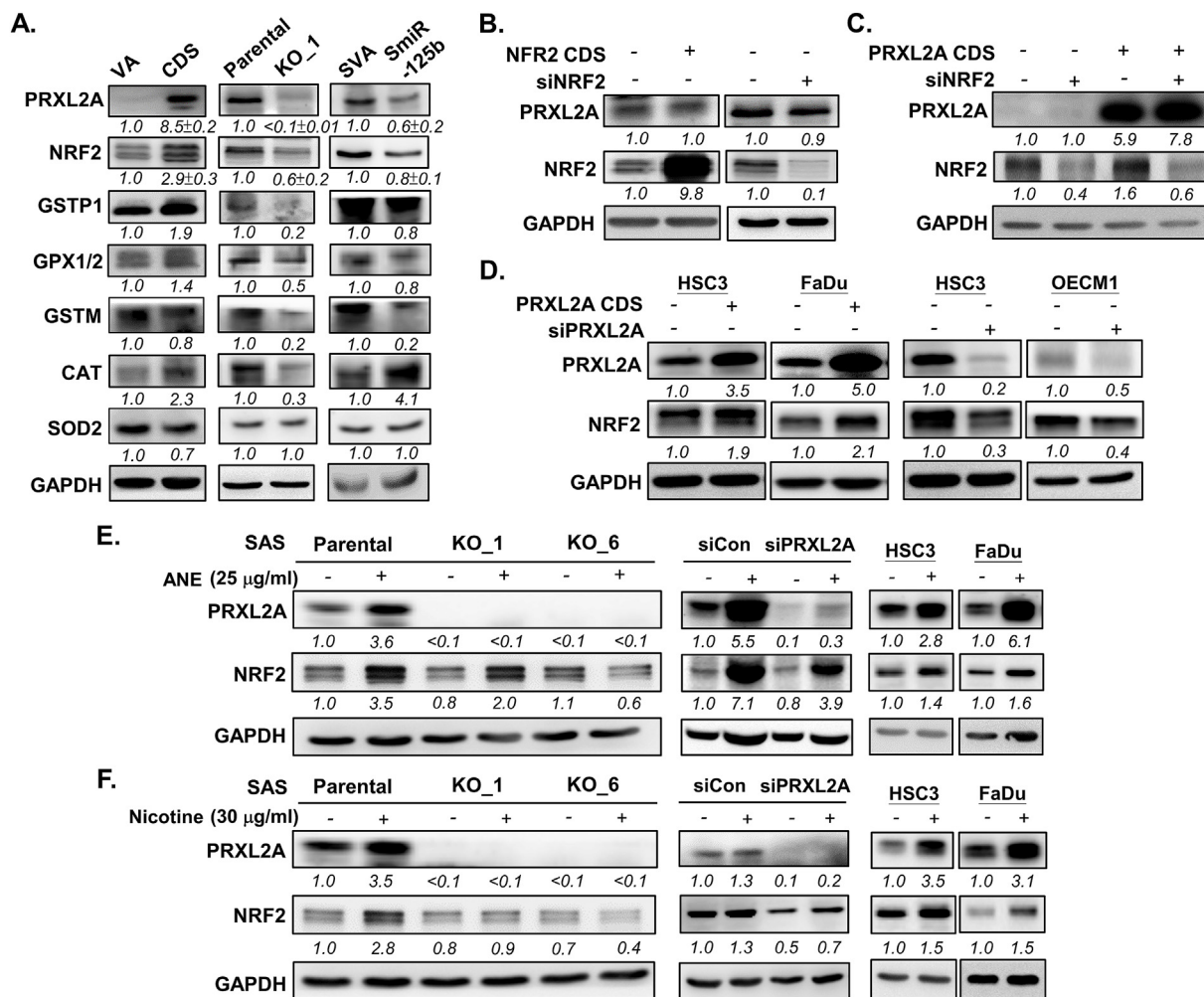


Fig. 5. NRF2 is downstream of PRXL2A. Western blot analysis. **A.** Analysis of the levels of antioxidative proteins in the CDS, KO_1 and *SmiR-125b* subclones relative to their controls. Consistent changes in GSTP1, GSPX1/2, and NRF2 secondary to the changes in PRXL2A and *miR-125b* expression can be seen across different subclones. **B.** NRF2 expression mediated by NRF2 CDS construct transfection and knockdown of NRF2 by siNRF2 oligonucleotide transfection are unable to alter the levels of PRXL2A in SAS cell. **C.** PRXL2A expression mediated by PRXL2A CDS construct transfection results in increased NRF2 expression, which can then be reduced by siNRF2 in SAS cell. The endogenous PRXL2A signals have been minimized in order to visualize the exogenous expression levels. **D.** Left, transient PRXL2A expression in HSC3 and FaDu cells increase NRF2 expression; Right, treatment with siPRXL2A in HSC3 and OECM1 cells decreases NRF2 expression. **E, F.** Cells treated with ANE and nicotine for 2 h. Left, SAS PRXL2A knockout subclones; Middle, SAS PRXL2A knockdown cells. The upregulation of NRF2 is mediated partly via PRXL2A based on the fact that knockout or knockdown of PRXL2A either abolishes or attenuates this upregulation. Right, HSC3 and FaDu cell lines. The treatment of ANE or nicotine upregulates both PRXL2A and NRF2. Numbers below pictures, normalized values. Data for PRXL2A and NRF2 in A. are mean \pm SE from quadruplicate analysis.

miR-125b and *miR-199a* expression by increasing the methylation of their promoter regions, which in turn activates upregulation of ERBB2 and ERBB3 resulting in tumor induction [28]. Inhibition of *miR-125b* also protected PC-12 cells from damage by ROS through the targeting of cystathionine β -synthase [50]. This study further links *miR-125b* downregulation to a decrease of ROS in OSCC cells. *miR-125b* seems to modulate ROS homeostasis by targeting the antioxidant PRXL2A. Taking this further, various other molecules, including DNMT1, TGF β and long noncoding RNAs, are known to be involved in the regulation of *miR-125b* expression in various different cell systems [28,51,52] and such signals/factors might also have a role in downregulating *miR-125b* in OSCC; this area needs to be explored in more detail.

Apart from the TCF12 signaling, which is also known to underlie high PRXL2A expression in tumors [6], we found in the present study that there is rapid upregulation of PRXL2A when cells are treated with various carcinogens. Functional assays showed that PRXL2A expression brings about increased oncogenicity, decreased intracellular ROS and lower CDDP sensitivity, while at the same time upregulating various antioxidants including GSTP1, GPX1/2, and NRF2 together. Since *miR-*

125b drives opposite influences, and that the activity and therapeutic efficacy modulated by *miR-125b* expression are attenuated by PRXL2A, the functional involvement of *miR-125b*-PRXL2A in OSCC pathogenesis is confirmed. In the expression and deletion subclones, we noted that the change in NRF2 expression was secondary to the expression of *miR-125b* and PRXL2A. By contrast, there was no reciprocal regulation by NRF2 of PRXL2A. Therefore, it seems likely that PRXL2A modulates pro-tumorigenic activity via NRF2 upregulation.

NRF2 transactivates *miR-125b* by binding to ARE in the *miR-125b* promoter to drive protection or oncogenesis in kidney, leukemia and corneal epithelium-derived progenitor cells [38–40]. The absence of NRF2 modulation on *miR-125b* expression due to the differences in transcriptional microenvironments in OSCC cells is suspected. In OSCC cells, upregulation of PRXL2A either by ectopic expression or oncogenic stimuli unequivocally results in the increased NRF2 expression. Like PRXL2A, the Parkinson's disease gene product DJ-1 peroxiredoxin-like peroxidase is also able to stabilize NRF2 in normal and malignant cells [53,54]. DJ-1 represses pTEN and is upregulated in malignancies including OSCC [55,56]. The potential involvement of DJ-1 in PRXL2A-

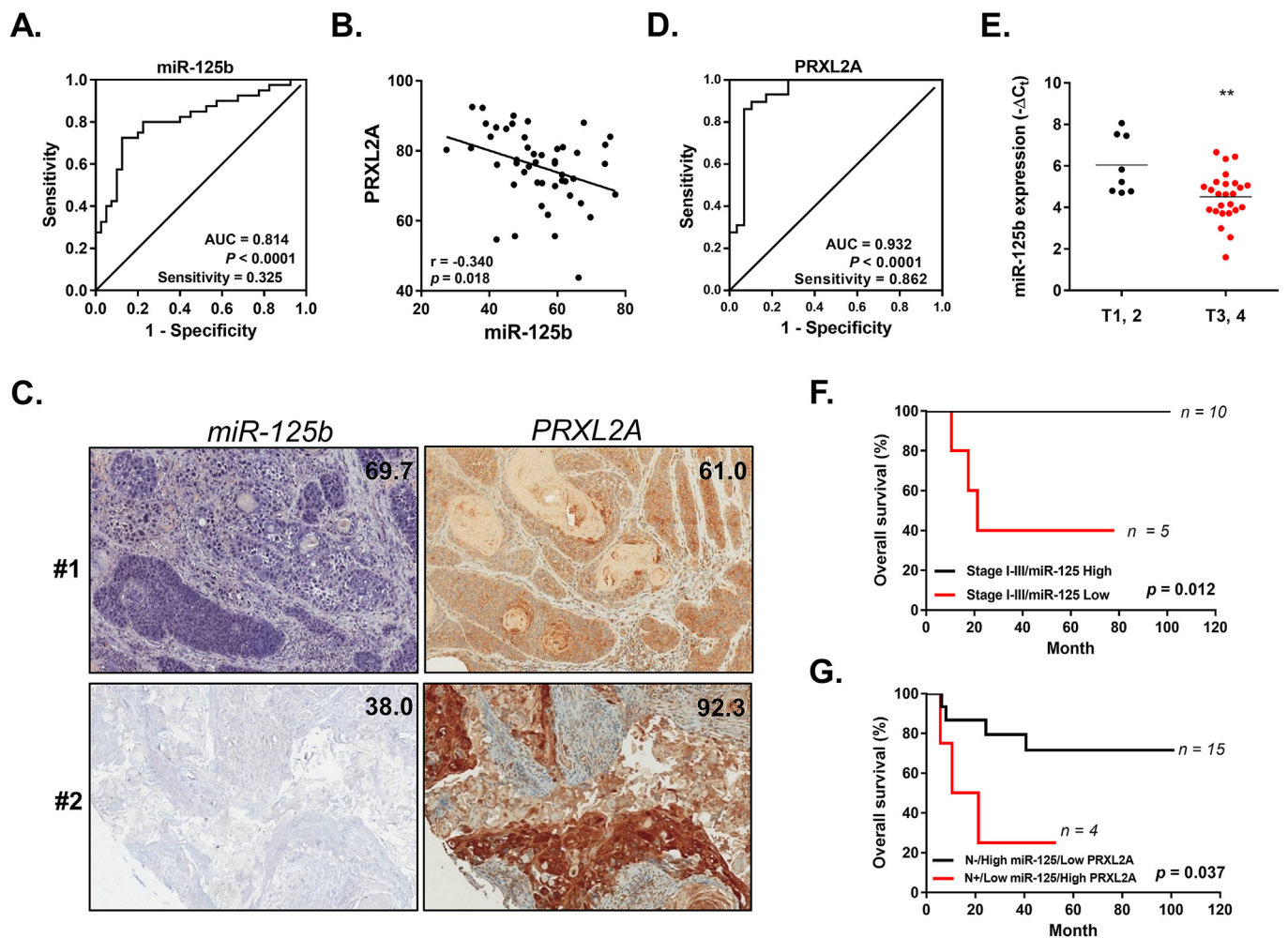


Fig. 6. PRXL2A and *miR-125b* expression in OSCC tissues are associated with patient survival. A, E. qPCR analysis of *miR-125b* in OSCC tissues. Others. ISH and IHC analysis of OSCC TMAs. A, D. ROC analysis. A. ROC analysis shows the strength of *miR-125b* expression can be used to distinguish OSCC samples from their NCMT samples. B. Correlation analysis. It shows a significantly reverse correlation between *miR-125b* pixel scores and PRXL2A pixel scores in OSCC tissues. C. Representative ISH and IHC images. Left, *miR-125b* staining; Right, PRXL2A immunoreactivity in tumors #1 and #2. Numbers in pictures, pixel scores. D. ROC analysis shows that the strength of PRXL2A immunoreactivity is able to distinguish OSCC samples from their NCMT samples. E. The *miR-125b* expression is significantly decreased in T3 and T4 tumors compared to T1 and T2 tumors. F, G. Survival analysis. F. Association between a lower level of *miR-125b* staining and a poorer survival rate among patients with stage I - III tumors. G. Patients with lower *miR-125b* expression and higher PRXL2A expression in tumors and nodal metastasis have very poor prognosis. N+, nodal metastasis.

associated NRF2 activation in OSCC needs addressing. Other pathophysiological regulation on PRXL2A-NRF2 remains to be specified. The decreased NRF2 following the knockdown of PRXL2A is remarkable in HSC3 and OECM1 cells. However, the *miR-125b* expression, the decreases of NRF2 in SAS cells depletion or knockdown of PRXL2A is much less. The findings raise concerns that NRF2 downregulation in SAS cells is more redundant in responses to PRXL2A downregulation relative to other OSCC cells. As SAS has profound NRF2 expression, it is presumable that NRF2 protein in SAS cell is highly stable and less degradable. It is also possible that the viability of SAS cell is relatively more sensitive to the change of NRF2 than other cells, and this sensitivity limits the extent of NRF2 downregulation. Nevertheless, further findings on the modulation effects of PRXL2A on NRF2 expression in OSCC cells would enable insights into how redox potential and ROS are associated with carcinogenesis. As NRF2 drives the expression of a panel of antioxidative or detoxification genes involved in redox homeostasis [57], any changes in GSTP1 and GPX1/2 expression should be considered to be downstream of the *miR-125b*-PRXL2A-NRF2 cascade [58].

As a whole, this study demonstrates that downregulation of the *miR-125b* suppressor molecule underlies PRXL2A upregulation in OSCC. The

lower levels of the *miR-125b*-PRXL2A-NRF2 regulation in OSCC seem to protect cancer cells from oxidative stress, thus increase CDDP resistance.

Conflicts of interest

The authors declared no conflict of interest.

Acknowledgments

This study was supported by Taipei Veterans General Hospital grant V106C-074, and grants MOST105-2314-B-010-027-MY3, MOST107-2314-B-010-032-MY3 and Postdoc Research Grants MOST105-2811-B-010-041, MOST106-2811-B-010-036 (for Dr. Yi-Fen Chen) from the Ministry of Science and Technology, Taiwan.

Appendix A. Supplementary data

Supplementary data to this article can be found online at <https://doi.org/10.1016/j.redox.2019.101140>.

References

- [1] C.J. Liu, T.Y. Liu, L.T. Kuo, H.W. Cheng, T.H. Chu, K.W. Chang, S.C. Lin, Differential gene expression signature between primary and metastatic head and neck squamous cell carcinoma, *J. Pathol.* 214 (4) (2008) 489–497.
- [2] S.Y. Kao, E. Lim, An overview of detection and screening of oral cancer in Taiwan, *Chin. J. Dent. Res.* 18 (1) (2015) 7–12.
- [3] E. Benson, R. Li, D. Eisele, C. Fakhry, The clinical impact of HPV tumor status upon head and neck squamous cell carcinomas, *Oral Oncol.* 50 (6) (2014) 565–574.
- [4] H.H. Lu, S.Y. Kao, T.Y. Liu, S.T. Liu, W.P. Huang, K.W. Chang, S.C. Lin, Areca nut extract induced oxidative stress and upregulated hypoxia inducing factor leading to autophagy in oral cancer cells, *Autophagy* 6 (6) (2010) 725–737.
- [5] F. Ganci, A. Sacconi, V. Manciocco, I. Sperduti, P. Battaglia, R. Covello, P. Muti, S. Strano, G. Spriano, G. Fontemaggi, G. Blandino, MicroRNA expression as predictor of local recurrence risk in oral squamous cell carcinoma, *Head Neck* 38 (Suppl 1) (2016) E189–E197.
- [6] Y.F. Chen, C.C. Yang, S.Y. Kao, C.J. Liu, S.C. Lin, K.W. Chang, MicroRNA-211 enhances the oncogenicity of actinogen-Induced oral carcinoma by repressing TCF12 and increasing antioxidant activity, *Cancer Res.* 76 (16) (2016) 4872–4886.
- [7] C.J. Liu, M.M. Tsai, P.S. Hung, S.Y. Kao, T.Y. Liu, K.J. Wu, S.H. Chiou, S.C. Lin, K.W. Chang, miR-31 ablates expression of the HIF regulatory factor FIH to activate the HIF pathway in head and neck carcinoma, *Cancer Res.* 70 (4) (2010) 1635–1644.
- [8] F. Jiang, W. Zhao, L. Zhou, Z. Liu, W. Li, D. Yu, MiR-222 targeted PUMA to improve sensitization of UMI cells to cisplatin, *Int. J. Mol. Sci.* 15 (12) (2014) 22128–22141.
- [9] A. Glasauer, N.S. Chandel, Targeting antioxidants for cancer therapy, *Biochem. Pharmacol.* 92 (1) (2014) 90–101.
- [10] G.Y. Liou, P. Storz, Reactive oxygen species in cancer, *Free Radic. Res.* 44 (5) (2010) 479–496.
- [11] X.J. Wang, Z. Sun, N.F. Villeneuve, S. Zhang, F. Zhao, Y. Li, W. Chen, X. Yi, W. Zheng, G.T. Wondrak, P.K. Wong, D.D. Zhang, Nrf2 enhances resistance of cancer cells to chemotherapeutic drugs, the dark side of Nrf2, *Carcinogenesis* 29 (6) (2008) 1235–1243.
- [12] L.J. Bao, M.C. Jaramillo, Z.B. Zhang, Y.X. Zheng, M. Yao, D.D. Zhang, X.F. Yi, Nrf2 induces cisplatin resistance through activation of autophagy in ovarian carcinoma, *Int. J. Clin. Exp. Pathol.* 7 (4) (2014) 1502–1513.
- [13] J.L. Roh, E.H. Kim, H. Jang, D. Shin, Nrf2 inhibition reverses the resistance of cisplatin-resistant head and neck cancer cells to artesunate-induced ferroptosis, *Redox. Biol.* 11 (2017) 254–262.
- [14] H. Cui, Y. Wang, Y. Wang, S. Qin, Genome-wide analysis of putative peroxiredoxin in unicellular and filamentous cyanobacteria, *BMC Evol. Biol.* 12 (2012) 220.
- [15] S.G. Rhee, H.A. Woo, I.S. Kil, S.H. Bae, Peroxiredoxin functions as a peroxidase and a regulator and sensor of local peroxides, *J. Biol. Chem.* 287 (7) (2012) 4403–4410.
- [16] Y. Yu, C. Zhang, G. Zhou, S. Wu, X. Qu, H. Wei, G. Xing, C. Dong, Y. Zhai, J. Wan, S. Ouyang, L. Li, S. Zhang, K. Zhou, Y. Zhang, C. Wu, F. He, Gene expression profiling in human fetal liver and identification of tissue- and developmental-stage-specific genes through compiled expression profiles and efficient cloning of full-length cDNAs, *Genome Res.* 11 (8) (2001) 1392–1403.
- [17] Y. Xu, L.R. Morse, R.A. da Silva, P.R. Odgren, H. Sasaki, P. Stashenko, R.A. Battaglini, PAMM: a redox regulatory protein that modulates osteoclast differentiation, *Antioxidants Redox Signal.* 13 (1) (2010) 27–37.
- [18] G. Valverde, H. Zhou, S. Lippold, C. de Filippo, K. Tang, D. Lopez Herraez, J. Li, M. Stoneking, A novel candidate region for genetic adaptation to high altitude in Andean populations, *PLoS One* 10 (5) (2015) e0125444.
- [19] P.S. Hung, C.J. Liu, C.S. Chou, S.Y. Kao, C.C. Yang, K.W. Chang, T.H. Chiu, S.C. Lin, miR-146a enhances the oncogenicity of oral carcinoma by concomitant targeting of the IRAK1, TRAF6 and NUMB genes, *PLoS One* 8 (11) (2013) e79926.
- [20] Y.M. Sun, K.Y. Lin, Y.Q. Chen, Diverse functions of miR-125 family in different cell contexts, *J. Hematol. Oncol.* 6 (2013) 6.
- [21] J. Banzhaf-Strathmann, D. Edbauer, Good guy or bad guy: the opposing roles of microRNA 125b in cancer, *Cell Commun. Signal.* 12 (2014) 30.
- [22] D. Wu, J. Ding, L. Wang, H. Pan, Z. Zhou, J. Zhou, P. Qu, microRNA-125b inhibits cell migration and invasion by targeting matrix metalloproteinase 13 in bladder cancer, *Oncol. Lett.* 5 (3) (2013) 829–834.
- [23] L. Huang, J. Luo, Q. Cai, Q. Pan, H. Zeng, Z. Guo, W. Dong, J. Huang, T. Lin, MicroRNA-125b suppresses the development of bladder cancer by targeting E2F3, *Int. J. Cancer* 128 (8) (2011) 1758–1769.
- [24] A. Feliciano, J. Castellvi, A. Artero-Castro, J.A. Leal, C. Romagosa, J. Hernandez-Losa, V. Peg, A. Fabra, F. Vidal, H. Kondoh, Y.C.S. Ramon, M.E. Leonart, miR-125b acts as a tumor suppressor in breast tumorigenesis via its novel direct targets ENPEP, CK2- α , CCNJ, and MEGF9, *PLoS One* 8 (10) (2013) e76247.
- [25] Y. Zhang, L.X. Yan, Q.N. Wu, Z.M. Du, J. Chen, D.Z. Liao, M.Y. Huang, J.H. Hou, Q.L. Wu, M.S. Zeng, W.L. Huang, Y.X. Zeng, J.Y. Shao, miR-125b is methylated and functions as a tumor suppressor by regulating the ETS1 proto-oncogene in human invasive breast cancer, *Cancer Res.* 71 (10) (2011) 3552–3562.
- [26] H.Y. Jia, Y.X. Wang, W.T. Yan, H.Y. Li, Y.Z. Tian, S.M. Wang, H.L. Zhao, MicroRNA-125b functions as a tumor suppressor in hepatocellular carcinoma cells, *Int. J. Mol. Sci.* 13 (7) (2012) 8762–8774.
- [27] J. Gong, J.P. Zhang, B. Li, C. Zeng, K. You, M.X. Chen, Y. Yuan, S.M. Zhuang, MicroRNA-125b promotes apoptosis by regulating the expression of Mcl-1, Bcl-w and IL-6R, *Oncogene* 32 (25) (2013) 3071–3079.
- [28] J. He, Q. Xu, Y. Jing, F. Agani, X. Qian, R. Carpenter, Q. Li, X.R. Wang, S.S. Peiper, Z. Lu, L.Z. Liu, B.H. Jiang, Reactive oxygen species regulate ERBB2 and ERBB3 expression via miR-199a/125b and DNA methylation, *EMBO Rep.* 13 (12) (2012) 1116–1122.
- [29] Y. Guan, H. Yao, Z. Zheng, G. Qiu, K. Sun, MiR-125b targets BCL3 and suppresses ovarian cancer proliferation, *Int. J. Cancer* 128 (10) (2011) 2274–2283.
- [30] J. Li, T. You, J. Jing, MiR-125b inhibits cell biological progression of Ewing's sarcoma by suppressing the PI3K/Akt signalling pathway, *Cell Prolif* 47 (2) (2014) 152–160.
- [31] F. Kong, C. Sun, Z. Wang, L. Han, D. Weng, Y. Lu, G. Chen, miR-125b confers resistance of ovarian cancer cells to cisplatin by targeting pro-apoptotic Bcl-2 antagonist killer 1, *J. Huazhong Univ. Sci. Technol. Med. Sci.* 31 (4) (2011) 543–549.
- [32] T.Z. Yuan, H.H. Zhang, X.L. Lin, J.X. Yu, Q.X. Yang, Y. Liang, J. Deng, L.J. Huang, X.P. Zhang, microRNA-125b reverses the multidrug resistance of nasopharyngeal carcinoma cells via targeting of Bcl-2, *Mol. Med. Rep.* 15 (4) (2017) 2223–2228.
- [33] W. Liu, J. Hu, K. Zhou, F. Chen, Z. Wang, B. Liao, Z. Dai, Y. Cao, J. Fan, J. Zhou, Serum exosomal miR-125b is a novel prognostic marker for hepatocellular carcinoma, *OncoTargets Ther.* 10 (2017) 3843–3851.
- [34] T. Zhu, W. Gao, X. Chen, Y. Zhang, M. Wu, P. Zhang, S. Wang, A pilot study of circulating microRNA-125b as a diagnostic and prognostic biomarker for epithelial ovarian cancer, *Int. J. Gynecol. Cancer* 27 (1) (2017) 3–10.
- [35] C.L. Nie, W.H. Ren, Y. Ma, J.S. Xi, B. Han, Circulating miR-125b as a biomarker of Ewing's sarcoma in Chinese children, *Genet. Mol. Res.* 14 (4) (2015) 19049–19056.
- [36] S.C. Peng, C.T. Liao, C.H. Peng, A.J. Cheng, S.J. Chen, C.G. Huang, W.P. Hsieh, T.C. Yen, MicroRNAs MiR-218, MiR-125b, and Let-7g predict prognosis in patients with oral cavity squamous cell carcinoma, *PLoS One* 9 (7) (2014) e102403.
- [37] H. Nakanishi, C. Taccioli, J. Palatini, C. Fernandez-Cymering, R. Cui, T. Kim, S. Volinia, C.M. Croce, Loss of miR-125b-1 contributes to head and neck cancer development by dysregulating TACSTD2 and MAPK pathway, *Oncogene* 33 (6) (2014) 702–712.
- [38] N.M. Shah, L. Zaitseva, K.M. Bowles, D.J. MacEwan, S.A. Rushworth, NRF2-driven miR-125B1 and miR-29B1 transcriptional regulation controls a novel anti-apoptotic miRNA regulatory network for AML survival, *Cell Death Differ.* 22 (4) (2015) 654–664.
- [39] M.S. Joo, C.G. Lee, J.H. Koo, S.G. Kim, miR-125b transcriptionally increased by Nrf2 inhibits AhR repressor, which protects kidney from cisplatin-induced injury, *Cell Death Dis.* 4 (2013) e899.
- [40] J. Zhou, L. Ge, C. Jia, X. Zheng, H. Cui, R. Zong, X. Bao, Y. Yin, J.X. Ma, W. Li, Z. Liu, Y. Zhou, ROS-mediated different homeostasis of murine corneal epithelial progenitor cell line under oxidative stress, *Sci. Rep.* 6 (2016) 36481.
- [41] K. Huang, S. Dong, W. Li, Z. Xie, The expression and regulation of microRNA-125b in cancers, *Acta Biochim. Biophys. Sin.* (Shanghai) 45 (10) (2013) 803–805.
- [42] W.A. Gonzalez-Arriagada, P. Olivero, B. Rodriguez, C. Lozano-Burgos, C.E. de Oliveira, R.D. Coletta, Clinicopathological significance of miR-26, miR-107, miR-125b, and miR-203 in head and neck carcinomas, *Oral Dis.* 24 (6) (2018) 930–939.
- [43] B.J. Henson, S. Bhattacharjee, D.M. O'Dee, E. Feingold, S.M. Gollin, Decreased expression of miR-125b and miR-100 in oral cancer cells contributes to malignancy, *Genes Chromosomes Cancer* 48 (7) (2009) 569–582.
- [44] S.H. Tseng, C.C. Yang, E.H. Yu, C. Chang, Y.S. Lee, C.J. Liu, K.W. Chang, S.C. Lin, K14-EGFP-miR-31 transgenic mice have high susceptibility to chemical-induced squamous cell tumorigenesis that is associating with Ku80 repression, *Int. J. Cancer* 136 (6) (2015) 1263–1275.
- [45] T.H. Chu, C.C. Yang, C.J. Liu, M.T. Lui, S.C. Lin, K.W. Chang, miR-211 promotes the progression of head and neck carcinomas by targeting TGF β RII, *Cancer Lett.* 337 (1) (2013) 115–124.
- [46] R. Marullo, E. Werner, N. Degtyareva, B. Moore, G. Altavilla, S.S. Ramalingam, P.W. Doetsch, Cisplatin induces a mitochondrial-ROS response that contributes to cytotoxicity depending on mitochondrial redox status and bioenergetic functions, *PLoS One* 8 (11) (2013) e81162.
- [47] D. Chen, R.J. Cabay, Y. Jin, A. Wang, Y. Lu, M. Shah-Khan, X. Zhou, MicroRNA deregulations in head and neck squamous cell carcinomas, *J. Oral Maxillofac. Res.* 4 (1) (2013) e2.
- [48] A. Tiwari, S. Shivananda, K.S. Gopinath, A. Kumar, MicroRNA-125a reduces proliferation and invasion of oral squamous cell carcinoma cells by targeting estrogen-related receptor alpha: implications for cancer therapeutics, *J. Biol. Chem.* 289 (46) (2014) 32276–32290.
- [49] S. Manca, A. Magrelli, S. Gialfi, K. Lefort, R. Ambra, M. Alimandi, G. Biolcati, D. Uccelletti, C. Pallechi, I. Screpanti, E. Candi, G. Melino, M. Salvatore, D. Tarascio, C. Talora, Oxidative stress activation of miR-125b is part of the molecular switch for Hailey-Hailey disease manifestation, *Exp. Dermatol.* 20 (11) (2011) 932–937.
- [50] Y. Shen, Z. Shen, L. Guo, Q. Zhang, Z. Wang, L. Miao, M. Wang, J. Wu, W. Guo, Y. Zhu, MiR-125b-5p is involved in oxygen and glucose deprivation injury in PC-12 cells via CBS/H2S pathway, *Nitric Oxide* 78 (2018) 11–21.
- [51] S. Ottaviani, J. Stebbing, A.E. Frampton, S. Zagorac, J. Krell, A. de Giorgio, S.M. Trabulo, V.T.M. Nguyen, L. Magnani, H. Feng, E. Giovannetti, N. Funel, T.M. Gress, L.R. Jiao, Y. Lombardo, N.R. Lemoine, C. Heeschen, L. Castellano, TGF- β induces miR-100 and miR-125b but blocks let-7a through LIN28B controlling PDAC progression, *Nat. Commun.* 9 (1) (2018) 1845.
- [52] C. Song, J. Wang, Y. Ma, Z. Yang, D. Dong, H. Li, J. Yang, Y. Huang, M. Plath, Y. Ma, H. Chen, Linc-smad7 promotes myoblast differentiation and muscle regeneration via sponging miR-125b, *Epigenetics* 13 (6) (2018) 591–604.
- [53] E. Andres-Mateos, C. Perier, L. Zhang, B. Blanchard-Fillion, T.M. Greco, B. Thomas, H.S. Ko, M. Sasaki, H. Ischiropoulos, S. Przedborski, T.M. Dawson, V.L. Dawson, DJ-1 gene deletion reveals that DJ-1 is an atypical peroxiredoxin-like peroxidase, *Proc. Natl. Acad. Sci. U. S. A.* 104 (37) (2007) 14807–14812.
- [54] C.M. Clements, R.S. McNally, B.J. Conti, T.W. Mak, J.P. Ting, DJ-1, a cancer- and Parkinson's disease-associated protein, stabilizes the antioxidant transcriptional master regulator Nrf2, *Proc. Natl. Acad. Sci. U. S. A.* 103 (41) (2006) 15091–15096.
- [55] R.H. Kim, M. Peters, Y. Jang, W. Shi, M. Pintilie, G.C. Fletcher, C. DeLuca, J. Liepa,

- L. Zhou, B. Snow, R.C. Binari, A.S. Manoukian, M.R. Bray, F.F. Liu, M.S. Tsao, T.W. Mak, DJ-1, a novel regulator of the tumor suppressor PTEN, *Cancer Cell* 7 (3) (2005) 263–273.
- [56] S. Xu, D. Ma, R. Zhuang, W. Sun, Y. Liu, J. Wen, L. Cui, DJ-1 Is upregulated in oral squamous cell carcinoma and promotes oral cancer cell proliferation and invasion, *J. Cancer* 7 (8) (2016) 1020–1028.
- [57] I.G. Ryoo, S.H. Lee, M.K. Kwak, Redox modulating NRF2: a potential mediator of cancer stem cell resistance, *Oxid. Med. Cell. Longev.* (2016) 2428153.
- [58] A.L. Furfaro, N. Traverso, C. Domenicotti, S. Piras, L. Moretta, U.M. Marinari, M.A. Pronzato, M. Nitti, The Nrf2/HO-1 Axis in cancer cell growth and chemoresistance, *Oxid. Med. Cell. Longev.* 2016 (2016) 1958174.